Intermetallic Compounds Formed during the Reflow and Aging of Sn-3.8Ag-0.7Cu and Sn-20In-2Ag-0.5Cu Solder Ball Grid Array Packages

M.D. CHENG,[1] S.Y. CHANG,[1] S.F. YEN,[1] and T.H. CHUANG[1,2]

1.—Institute of Materials Science and Engineering, National Taiwan University, Taipei 106, Taiwan.
2.—E-mail: tunghan@ccms.ntu.edu.tw

After reflow of Sn-3.8Ag-0.7Cu and Sn-20In-2Ag-0.5Cu solder balls on Au/Ni surface finishes in ball grid array (BGA) packages, scallop-shaped intermetallic compounds $(Cu_{0.70}Ni_{0.28}Au_{0.02})_6Sn_5$ (IM1a) and $(Cu_{0.76}Ni_{0.24})_6(Sn_{0.86}In_{0.14})_5$ (IM1b), respectively, appear at the interfaces. Aging at 100°C and 150°C for Sn-3.8Ag-0.7Cu results in the formation of a new intermetallic phase $(Cu_{0.70}Ni_{0.14}Au_{0.16})_6Sn_5$ (IM2a) ahead of the former IM1a intermetallics. The growth of the newly appeared intermetallic compound, IM2a, is governed by a parabolic relation with an increase in aging time, with a slight diminution of the former IM1a intermetallics. After prolonged aging at 150°C, the IM2a intermetallics partially spall off and float into the solder matrix. Throughout the aging of Sn-20In-2Ag-.5Cu solder joints at 75°C and 115°C, partial spalling of the IM1b interfacial intermetallics induces a very slow increase in thickness. During aging at 115°C for 700 h through 1,000 h, the spalled IM1b intermetallics in the solder matrix migrate back to the interfaces and join with the IM1b interfacial intermetallics to react with the Ni layers of the Au/Ni surface finishes, resulting in the formation and rapid growth of a new $(Ni_{0.85}Cu_{0.15})(Sn_{0.71}In_{0.29})_2$ intermetallic layer (IM2b). From ball shear tests, the strengths of the Sn-3.8Ag-0.7Cu and Sn-20In-2Ag-0.5Cu solder joints after reflow are ascertained to be 10.4 N and 5.4 N, respectively, which drop to lower values after aging.

Key words: Sn-3.8Ag-0.7Cu, Sn-20In-2Ag-0.5Cu, Au/Ni surface finish, ball grid array package, reflow, aging, intermetallic compounds

INTRODUCTION

Owing to the advantages of good wettability, improved creep resistance, and long thermal fatigue life, the Sn-Ag-Cu alloy has been recommended by the National Electronics Manufacturing Initiative to replace the eutectic Sn-Pb solder in reflow processing.[1] However, the high melting point of this alloy system (e.g., 218°C for an Sn-3.8Ag-0.7Cu solder versus 183°C for the traditional eutectic Sn-37Pb solder) impedes its applicability in electronic packaging.

Gold/nickel metallization layers have been widely used as the surface finishes for Cu pads in ball grid array (BGA) packaging.[2] Regrettably, Au thin films can dissolve rapidly into the Sn-Pb solder balls of BGA packages to form $AuSn_4$ intermetallic compounds.[3–6] Subsequent aging treatments cause the $AuSn_4$ intermetallics in the solder matrix to migrate to the solder ball/pad interfaces and react with the Ni metallization, leading to the formation of a continuous $(Au,Ni)Sn_4$ intermetallic layer.[4–6] The existence of a brittle $(Au,Ni)Sn_4$ layer at the interfaces is the reason for the decrease in the strength of BGA solder joints.[6]

During the reflow and aging of the solder joints, intermetallic transformation occurs at the interfaces and in the solder interior, which exerts an influence on the bonding effect and solder strength. Kim et al. showed that the interfacial reactions

(Received May 16, 2003; accepted September 4, 2003)

between Sn-Pb and Ni gave rise to the formation of Ni_3Sn_4.[7] However, Zeng et al. indicated that the formation of Ni_3Sn_4 was suppressed by the presence of Cu in Sn-Ag-Cu solder, and $(Cu,Ni)_6Sn_5$ intermetallic compounds appeared at the SnAgCu/Ni interfaces instead.[8] A similar result was obtained by Zhang et al.: $(Cu,Ni)_6Sn_5$ intermetallic compounds formed during the interfacial reactions between Sn-3.5Ag-1.0Cu solder bumps and Al/Ni(V)/Cu under bump metallizations in the flip-chip assembly.[9] For the reflow and aging of Sn-4Ag-0.5Cu and Sn-3.5Ag-0.75Cu solders on Au/Ni surface finishes in BGA packages, Shiau et al. reported that $(Cu,Ni,Au)_6Sn_5$ intermetallic compounds appeared at the solder/pad interfaces.[10]

Although Zeng et al.[8] reported that Ag was not directly involved in the interfacial reactions between the SnAgCu solder and Ni, the mechanical strength of Sn-based solders can be increased by adding Ag to form Ag_3Sn precipitates in the solder matrix.[11] In certain cases, however, the appearance of large Ag_3Sn intermetallic plates in the solder matrix can be detrimental to the mechanical properties of the solder joints,[12] such as their fatigue resistance.[13]

Indium has been added into solder alloys as a melting-point depressant. An indium-containing solder has also been shown to possess improved wettability, ductility, and fatigue resistance.[14,15] The addition of indium into Sn-based solders facilitates the formation of an $AuIn_2$ intermetallic layer at the solder/pad interface, capable of inhibiting Au dissolution into the solder matrix to generate the brittle $AuSn_4$ phase.[16] Lee found that failure in In-Sn solder joints caused by Au embrittlement can be curtailed because of the lower solubility of Au in In-Sn alloys.[17]

In this present study, indium is added into a Sn-Ag-Cu solder for the purpose of lowering the melting temperature and preventing Au embrittlement of BGA packages. The intermetallic compounds formed during reflow and aging for both Sn-3.8Ag-0.7Cu and Sn-20In-2Ag-0.5Cu are analyzed. In addition, the ball shear strengths of the solder joints correlated with intermetallic formation are also investigated.

EXPERIMENTAL

The BGA packages, whose geometry was defined previously,[18] contain a silicon die (size: 4.5 mm × 4.5 mm × 0.25 mm) attached to a bismaleimide-triazine resin substrate and encapsulated in a molding compound. Each package was fitted with 49 Cu pads electroplated with 10-μm-thick Ni and 0.7-μm-thick Au. The Sn-3.8Ag-0.7Cu and Sn-20In-2Ag-0.5Cu (wt.%) solder balls of 0.4-mm diameter were dipped in flux, placed on the Au/Ni surface finishes of Cu pads, and then heated in a hot-air reflow furnace equipped with five heating zones. The reflow temperature profiles for the BGA specimens of both solders are plotted in Fig. 1. Differential scanning calorimetry analysis showed the solidus and liquidus temperatures of the Sn-20In-2Ag-0.5Cu solder at 165.6°C and 179.5°C, respectively, while Sn-3.8Ag-0.7Cu had a eutectic point of 217.8°C. It is evident that the Sn-20In-2Ag-0.5Cu solder possessed much lower melting temperatures than the Sn-3.8Ag-0.7Cu solder. As compared to a Sn-20In-0.8Cu solder (solidus: 168.3°C, liquidus: 185.4°C) reported in a previous work of ours,[19] Sn-20In-2Ag-0.5Cu also showed a slightly lower melting temperature. When the temperature rose above the melting point of Sn-3.8Ag-0.7Cu, liquid solder reactions took place at the interfaces between solder balls and Au/Ni surface finishes. After reflow, aging treatments were performed at various temperatures (Sn-3.8Ag-0.7Cu: 100°C and 150°C, Sn-20In-2Ag-0.5Cu: 75°C and 115°C) for various times, ranging from 100 h to 1,000 h. All samples were cross-sectioned through a row of solder balls, ground with 1,500-grit SiC paper, and polished with 0.3-μm Al_2O_3 powder. The morphology of the intermetallic compounds was observed by scanning electron microscopy (SEM), and their chemical compositions were analyzed by energy dispersive x-ray spectrometry (EDX).

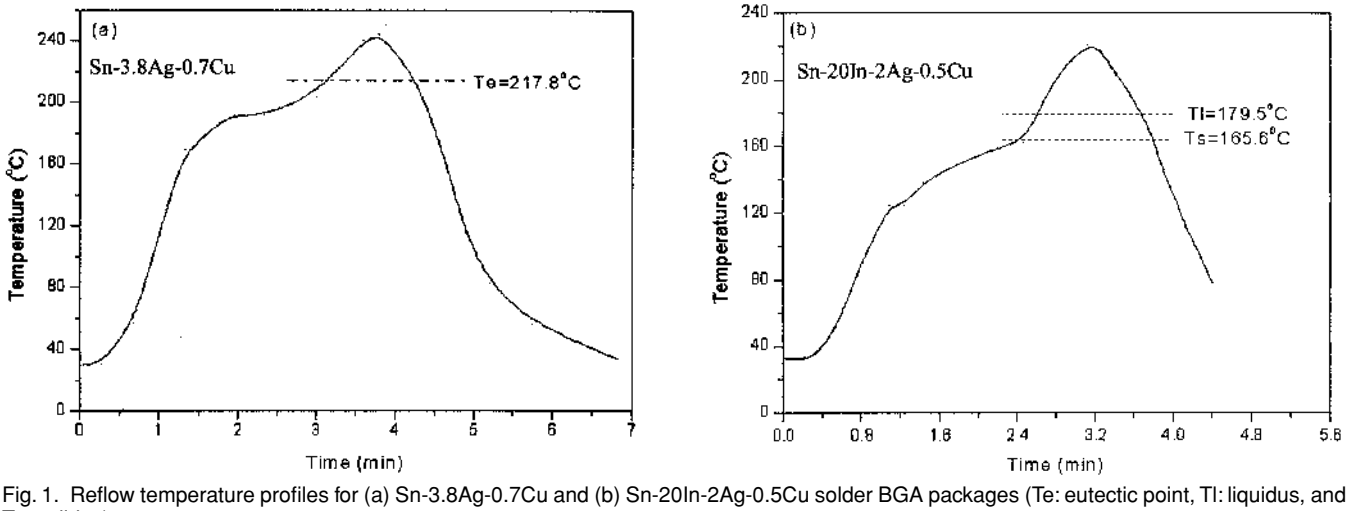

Fig. 1. Reflow temperature profiles for (a) Sn-3.8Ag-0.7Cu and (b) Sn-20In-2Ag-0.5Cu solder BGA packages (Te: eutectic point, Tl: liquidus, and Ts: solidus).

The bonding strength of solder balls on Au/Ni/Cu pads under various heating conditions were measured via ball shear tests. The measurements were taken at a shear rate of 0.1 mm/sec and a shear height of 80 μm (about 1/4 of the reflowed ball height). After ball shear testing, fractography was performed on the solder joints using SEM.

RESULTS AND DISCUSSION

Figure 2 shows the microstructure of Sn-3.8Ag-0.7Cu solder balls before reflow on the Au/Ni surface finishes, where Ag_3Sn (shown in white) and Cu_6Sn_5 (in gray) precipitates are embedded in the Sn-rich matrix. The composition (wt.%) of the solder matrix as analyzed by EDX is Sn-0.8Ag-0.7Cu. The formation of Ag_3Sn precipitates is the reason for the large deviation of Ag content from that within the solder alloy (3.8wt.% Ag), when one Sn atom can exhaust three Ag atoms during the precipitation reaction. The Cu content of the solder matrix was not affected by the precipitation of the Cu_6Sn_5 intermetallic phase.

Figure 3 shows the decreased amount of Cu_6Sn_5 in the solder matrix after reflow. Instead, scallop-shaped intermetallic compounds (IM1a) have appeared at the interfaces between solder balls and Au/Ni surface finishes of Cu pads. The EDX analysis shows that the composition (at.%) of the interfacial intermetallics is Cu:Ni:Au:Sn = 39.74:16.09:1.09:43.08, which corresponds to the $(Cu_{0.70}Ni_{0.28}Au_{0.02})_6Sn_5$ phase. The Ni layer acts as a diffusion barrier during reflow; the Cu atoms in the Au/Ni/Cu pads are incapable of outward floating to react with the Sn-3.8Ag-0.7Cu solder. Therefore, the formation of the $(Cu_{0.70}Ni_{0.28}Au_{0.02})_6Sn_5$ intermetallic compounds (IM1a) are attributed to partial dissolution of the Cu_6Sn_5 precipitates in the solder matrix, when Cu is released to react with the Au and Ni layers at the solder/pad interface.

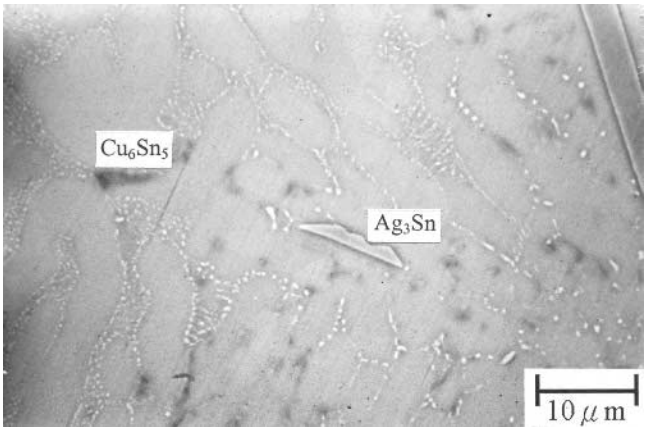

Fig. 2. Microstructure of the Sn-3.8Ag-0.7Cu solder ball prior to reflow.

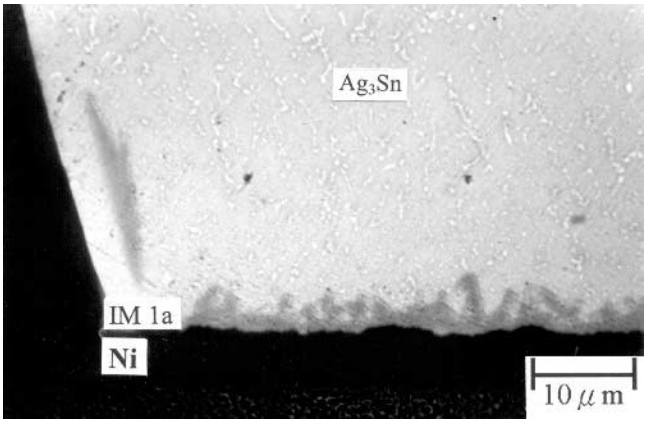

Fig. 3. Morphology of intermetallic compounds formed at the interfaces between the as-reflowed Sn-3.8Ag-0.7Cu solder balls and the Au/Ni surface finishes of Cu pads.

Figures 4 and 5, respectively, show drastic decreases of Cu_6Sn_5 precipitates in the solder matrix resulting from aging of the reflowed specimens conducted at 100°C and 150°C. However, the interfacial-intermetallic compounds (IM1a) formed during reflow have not grown with aging time. Instead, a new intermetallic phase (IM2a) appears at the front of the original intermetallic scallops (IM1a). The EDX analysis identifies the composition (at.%) of the newly appeared intermetallic compound as Cu:Ni:Au:Sn 5 39.58:7.66:8.62:44.15, which corresponds to the $(Cu_{0.70}Ni_{0.14}Au_{0.16})_6Sn_5$ phase. The compositions of IM1a and IM2a intermetallics remain constant throughout various aging treatments, i.e., they are independent of the aging temperatures and times.

Figure 4 shows that the Ag_3Sn fine particles distribute uniformly in the solder matrix during aging at 100°C, accompanied with the dissolution of Cu_6Sn_5 precipitates. These Ag_3Sn precipitates grow only slightly with an increase of the aging time at such a low temperature. However, as the aging temperature increases from 100°C to 150°C, the size of the Ag_3Sn precipitates increases, as shown in Fig. 5. At this high temperature, these precipitates coarsened drastically with an increase in aging time. Figure 5 shows that the number of Ag_3Sn particles decreased as the solder coarsened.

The thicknesses of interfacial intermetallics (IM1a and IM2a) formed during the reflow and aging are measured and listed in Table I. The intermetallic compounds IM1a previously formed after reflow have diminished slightly during the aging process, while the newly appeared IM2a phase grows at a more rapid pace. Some IM1a compounds transformed into IM2a, and more Cu_6Sn_5 precipitates in the solder matrix dissolved to react with Au and Ni, which explains the rapid growth of IM2a. The log thicknesses of IM2a formed during the 150°C aging for various reaction times (t) are plotted versus log t, as shown in Fig. 6. An n value of 0.51 for the kinetic relation ($x = t^n$) is derived from the slope of the plot, which indicates that the growth of the IM2a intermetallic compound at the interfaces during aging is diffusion-controlled.

In Fig. 5, IM2a intermetallic compounds are found to partially spall from the interfaces and float into the solder matrix after prolonged aging. The spalling of $(Cu_{0.70}Ni_{0.14}Au_{0.16})_6Sn_5$ intermetallic

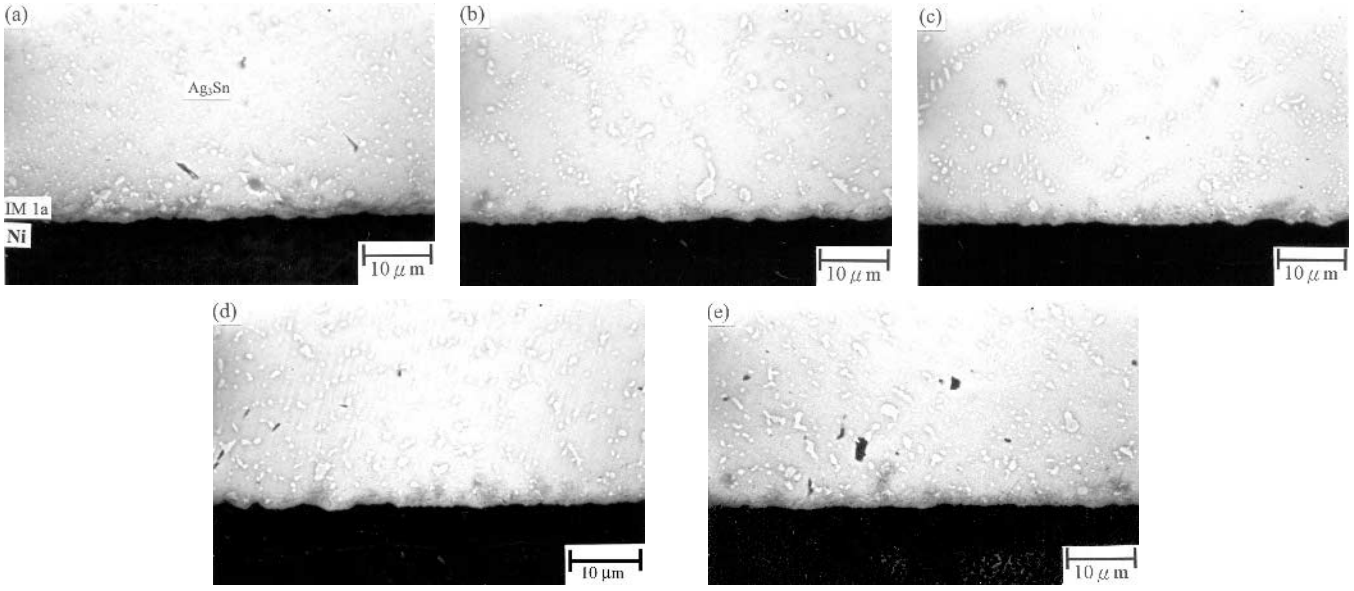

Fig. 4. Morphology of intermetallic compounds formed at the interfaces between Sn-3.8Ag-0.7Cu solder balls and Au/Ni surface finishes of Cu pads after aging at 100°C for various times: (a) 100 h, (b) 300 h, (c) 500 h, (d) 700 h, and (e) 1,000 h.

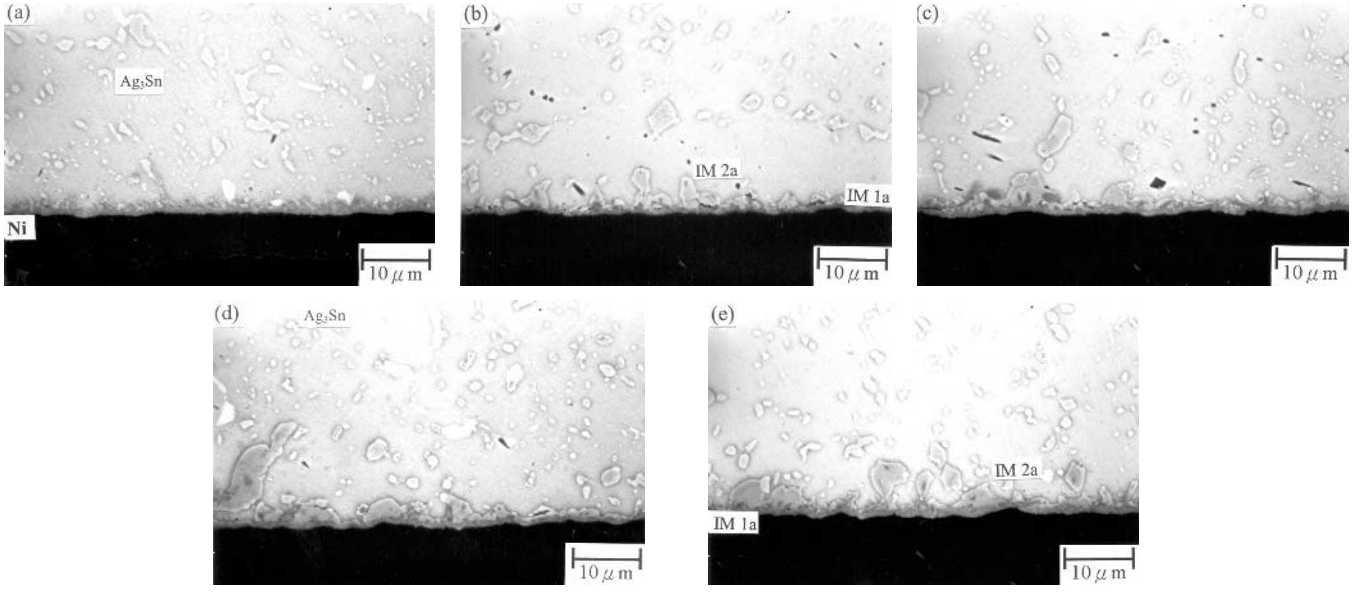

Fig. 5. Morphology of intermetallic compounds formed at the interfaces between Sn-3.8Ag-0.7Cu solder balls and Au/Ni surface finishes of Cu pads after aging at 150°C for various times: (a) 100 h, (b) 300 h, (c) 500 h, (d) 700 h, and (e) 1,000 h.

Table I. Thicknesses of Intermetallic Compounds Formed during the Reflow and Aging of Sn-3.8Ag-0.7Cu and Sn-20In-2Ag-0.5Cu Solder Balls with Au/Ni Surface Finishes of Cu Pads in Ball Grid Array Packages

	Thickness (μm)					
	Sn-3.8Ag-0.7Cu			Sn-20In-2Ag-0.5Cu		
Aging Time (h)	IM1a (100°C)	IM1a (150°C)	IM2a (150°C)	IM1b (75°C)	IM1b (115°C)	IM2b (115°C)
As reflow	2.26	2.26	0	1.82	1.82	0
100	2.11	1.77	0.57	1.95	3.51	0
300	1.94	1.46	0.72	2.01	3.58	0.22
500	2.11	1.41	0.93	2.08	3.62	0.87
700	1.99	1.38	1.09	2.12	2.99	7.97
1,000	1.94	1.35	1.35	2.16	1.90	14.42

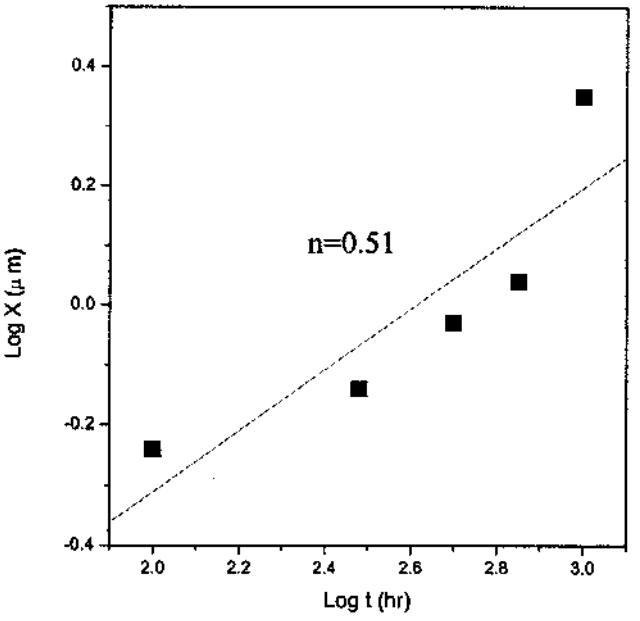

Fig. 6. Log plots for the thickness of the interfacial $(Cu_{0.70}Ni_{0.14}Au_{0.16})_6Sn_5$ intermetallic compounds formed during aging of Sn-3.8Ag-0.7Cu BGA packages at 150°C.

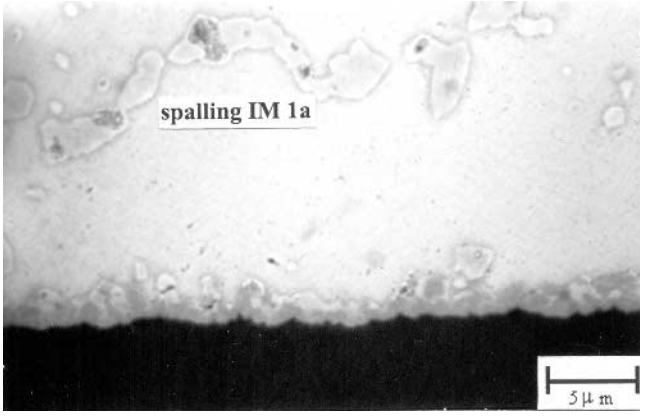

Fig. 7. Spalling of $(Cu_{0.70}Ni_{0.14}Au_{0.16})_6Sn_5$ intermetallic compounds from the interfaces after aging of the Sn-3.8Ag-0.7Cu BGA package at 150°C for 700 h.

compounds (IM2a) can be clearly observed in Fig. 7, while the $(Cu_{0.70}Ni_{0.28}Au_{0.02})_6Sn_5$ intermetallic compounds (IM1a) stay at the interface. As the IM2a intermetallics spall and float into the solder matrix, they join with the coarsened Ag_3Sn precipitates to form intermetallic chains or clusters, as shown by Fig. 8.

Prior to reflow, the Sn-20In-2Ag-0.5Cu solder consists of $Cu_6(Sn_{0.64}In_{0.36})_5$ and Ag_2In precipitates embedded in the Sn-rich matrix, as shown in Fig. 9. The EDX analysis identifies the composition (wt.%) of the solder matrix as Sn:In:Ag:Cu = 78.91:18.43:1.78:0.88. The In and Ag contents here are less than what were originally within the Sn-20In-2Ag-0.5Cu alloy because of the formation of the Ag_2In phase. The Cu content of the solder matrix increases slightly from 0.50 wt.% to 0.88 wt.% because the Ag_2In precipitates far exceed the Cu_6 $(Sn_{0.64}In_{0.36})_5$ in numbers.

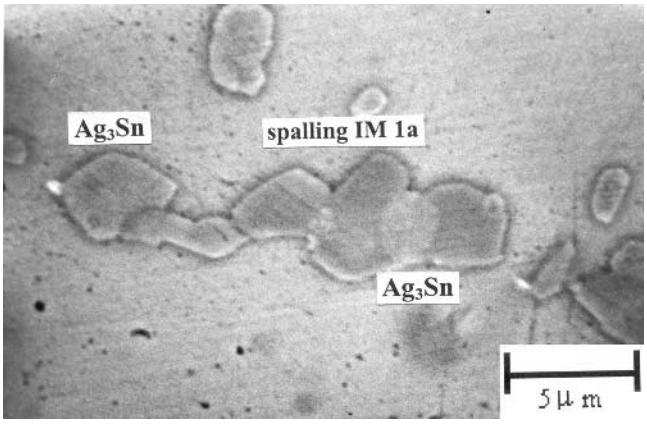

Fig. 8. Combination of spalled $(Cu_{0.70}Ni_{0.14}Au_{0.16})_6Sn_5$ intermetallic compounds with coarsened Ag_3Sn precipitates in the solder matrix to form intermetallic chains after aging of the Sn-3.8Ag-0.7Cu BGA package at 150°C for 1,000 h.

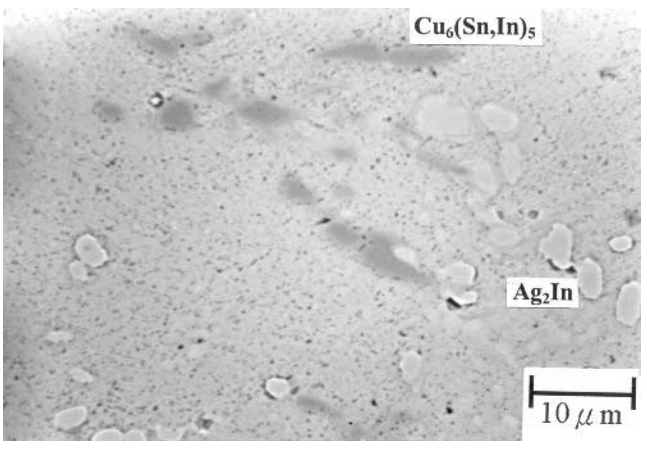

Fig. 9. Microstructure of the Sn-20In-2Ag-0.5Cu solder before reflow.

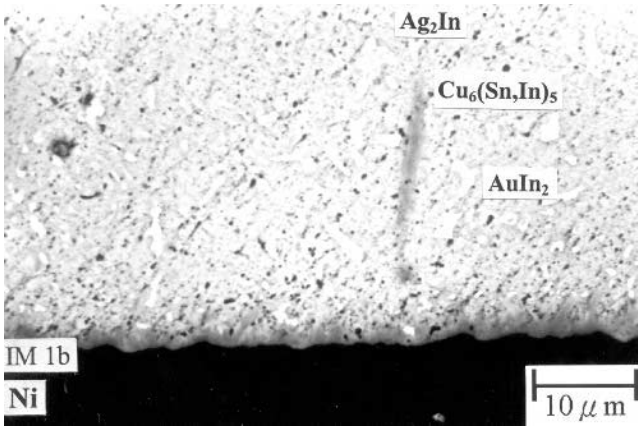

Fig. 10. Morphology of the intermetallic compounds formed at the interfaces between Sn-20In-2Ag-0.5Cu solder balls and Au/Ni surface finishes of BGA packages. IM1b: $(Cu_{0.76}Ni_{0.24})_6(Sn_{0.86}In_{0.14})_5$.

Figure 10 shows the microstructure of a Sn-20In-2Ag-0.5Cu solder ball after reflow. There is a significant decrease in the amount of the $Cu_6(Sn_{0.64}In_{0.36})_5$ precipitates in the solder matrix. Along with the diminishing of $Cu_6(Sn_{0.64}In_{0.36})_5$ in the solder matrix, scallop-shaped intermetallic compounds (IM1b) have appeared at the interfaces between solder balls

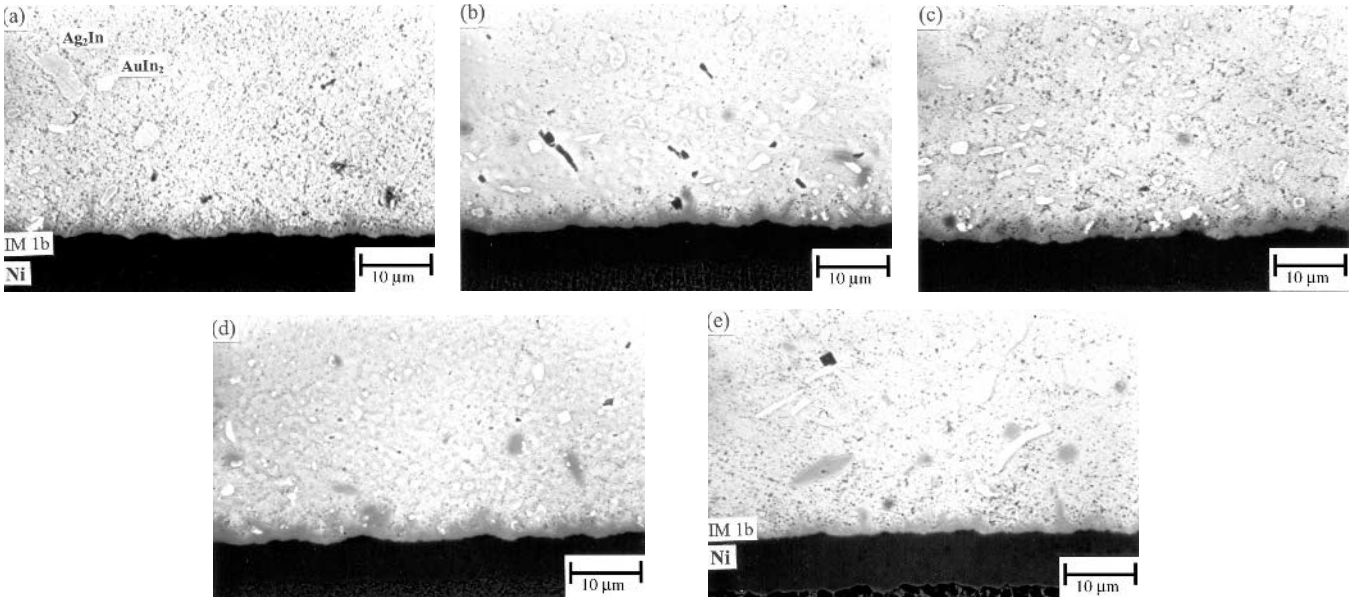

Fig. 11. Microstructure of the intermetallic compounds formed during the aging of Sn-20In-2Ag-0.5Cu BGA packages with Au/Ni surface finishes at 75°C for various times: (a) 100 h, (b) 300 h, (c) 500 h, (d) 700 h, and (e) 1,000 h.

and Au/Ni surface finishes. The composition (at.%) of these interfacial intermetallics is Cu:Ni:Sn:In = 40.61:13.06:39.79:6.54, which corresponds to the $(Cu_{0.76}Ni_{0.24})_6(Sn_{0.86}In_{0.14})_5$ phase. The formation of IM1b intermetallic compounds at the solder/pad interfaces is attributed to the dissolution of $Cu_6(Sn_{0.64}In_{0.36})_5$ precipitates in the solder matrix, as the Cu atoms are released to react with the Au/Ni surface finishes. Figure 10 also shows $AuIn_2$ intermetallic compounds (shown in white) appear in large quantities in the solder matrix. The composition (wt.%) of the solder matrix after reflow as analyzed by EDS is Sn:In:Ag:Cu = 76.67:20.74:1.77:0.82, which is nearly the same as it was prior to reflow.

Aging the Sn-20In-2Ag-0.5Cu BGA packages at 75°C yield a slight growth of IM1b intermetallics at the interfaces between solder balls and Au/Ni surface finishes with an increase of aging time from 100 h to 1,000 h, as shown by Fig. 11. The Ag_2In and $Cu_6(Sn_{0.64}In_{0.36})_5$ precipitates distribute uniformly in the solder matrix. Figure 11 shows that the IM1b intermetallic compounds have partially spalled from the interfaces and floated into the solder matrix. The very slow increase in IM1b thickness as a result of spalling is also listed in Table I.

Figure 12 shows that a thicker, IM1b interfacial-intermetallic layer can be obtained for the aging durations below 500 h with the aging temperature increased to 115°C, as compared with the result obtained at 75°C. However, Table I and Fig. 13 indicate that, similar to the IM1b growth at 75°C, the IM1b intermetallics also grow at a slow rate at 115°C because of the spalling effect on the intermetallics. After prolonged aging at 115°C, a new intermetallic layer (IM2b) appears at the interface between IM1b intermetallic compounds and the Au/Ni surface finish. The EDX analysis identifies the composition (at.%) of IM2b as Ni:Cu:Sn:In = 29.37:5.38:46.08:19.18, which corresponds to the $(Ni_{0.85}Cu_{0.15})(Sn_{0.71}In_{0.29})_2$ phase. Such an intermetallic phase is consistent with the findings in our previous study on the interfacial reactions between liquid In-49Sn solders and Ni substrates at temperatures ranging from 150°C to 300°C, when a $Ni_{33}Sn_{48.5}In_{18.5}$ intermetallic compound was identified during In-49Sn/Ni soldering reactions and its corresponding $Ni(Sn_{0.72}In_{0.28})_2$ phase ascertained.[20] Although neither $NiSn_2$ nor $NiIn_2$ has been reported in the Ni-Sn and Ni-In binary phase diagrams, a phase equilibrium Ni $(Sn_{0.72}In_{0.28})_2$ can be surmised to exist in the Ni-Sn-In ternary phase diagram at a temperature below 300°C.

Figure 12 also reveals the diminution of the original IM1b intermetallics along with the growth of the IM2b intermetallic layers. However, the growth rate of IM2b is much greater than the diminishing rate of IM1b, as indicated by Fig. 13. The result implies that the rapid growth of IM2b is not caused by the reactions between IM1b interfacial intermetallics and the Ni layer of the Au/Ni surface finishes. An interesting phenomenon is noted in Fig. 12d and e: the spalling of the IM1b intermetallics in the solder matrix also subsides ostensibly along with the IM2b growth. The spalled IM1b intermetallics migrated back from the solder matrix and joined the IM1b interfacial intermetallics to react with the Ni layers of Au/Ni surface finishes, leading to the dramatic increase in IM2b thickness. In a previous study on the reflow and aging of Sn-20In-0.8Cu BGA packages,[19] an additional intermetallic compound $(Ni_{0.91}Cu_{0.09})_3(Sn_{0.77}In_{0.23})_2$ was found in front of the Ni layer after aging at 115°C for 750 h, whose growth was much slower compared to the $(Ni_{0.85}Cu_{0.15})(Sn_{0.71}In_{0.29})_2$ intermetallic layer in the current case.

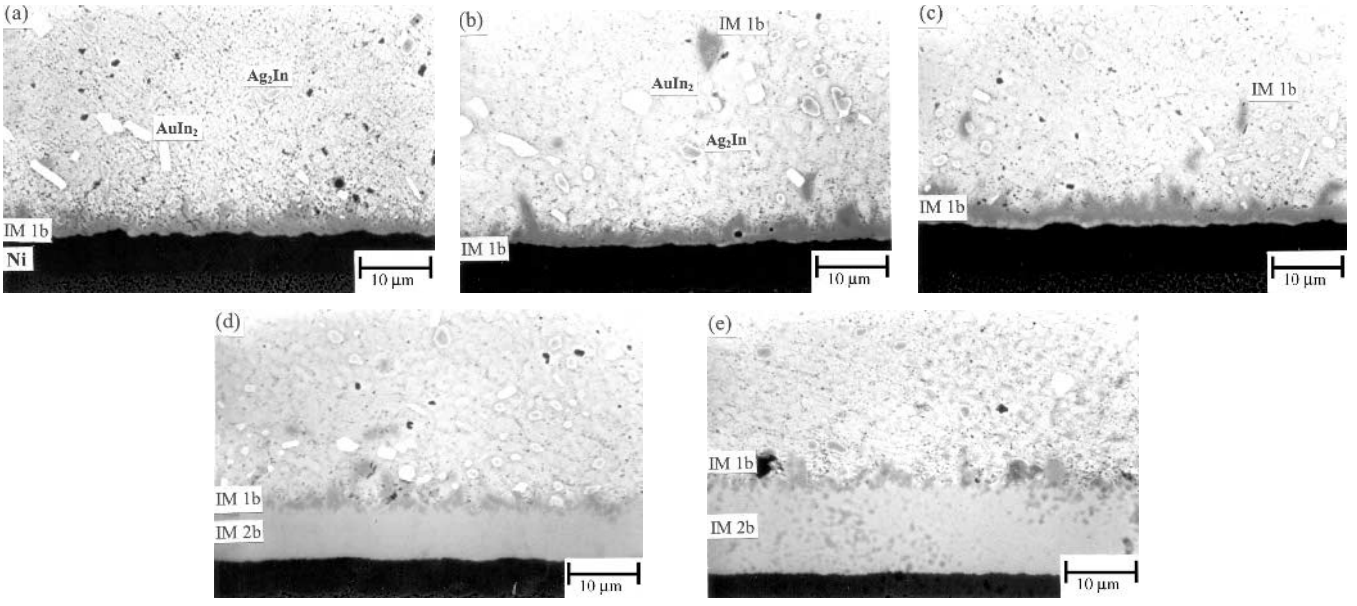

Fig. 12. Microstructure of the intermetallic compounds formed during the aging of Sn-20In-2Ag-0.5Cu BGA packages with Au/Ni surface finishes at 115°C for various times: (a) 100 h, (b) 300 h, (c) 500 h, (d) 700 h, and (e) 1,000 h. IM2: $(Ni_{0.85}Cu_{0.15})(Sn_{0.71}In_{0.29})_2$.

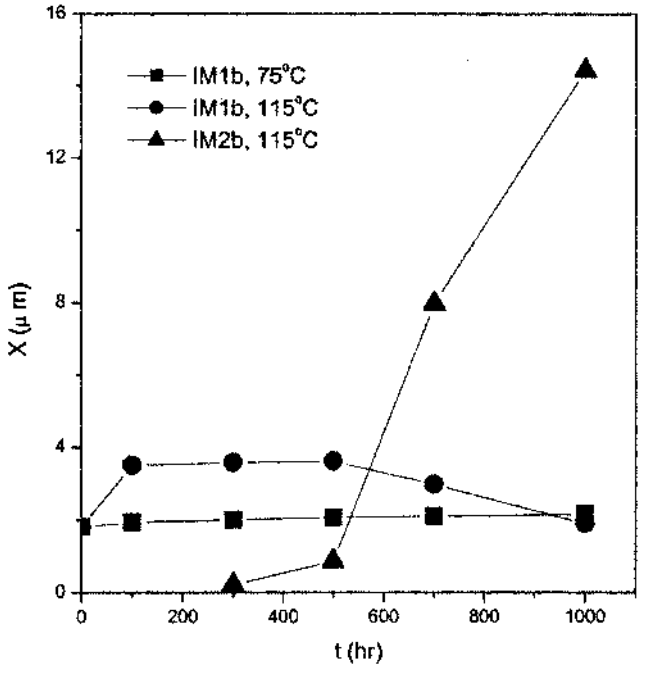

Fig. 13. Thicknesses of the intermetallic compounds grown at the interfaces between Sn-20In-2Ag-0.5Cu solder balls and Au/Ni surface finishes of BGA packages after aging at 75°C and 115°C for various times.

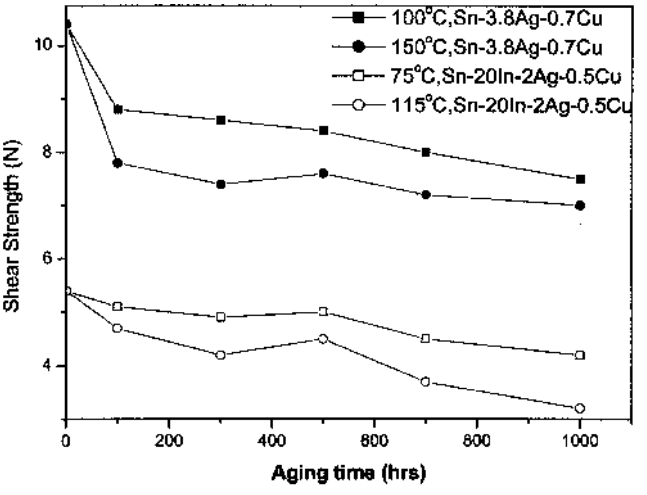

Fig. 14. Ball shear strengths of the Sn-3.8Ag-0.7Cu and Sn-20In-2Ag-0.5Cu BGA packages under various aging conditions.

The ball shear strengths of Sn-3.8Ag-0.7Cu and Sn-20In-2Ag-0.5Cu solder joints in BGA packaging after reflow and aging treatments under various conditions are listed in Table II, and the results are plotted in Fig. 14. The as-reflowed Sn-3.8Ag-0.7Cu solder joints possess a high strength of 10.4 N, which is about double the strength of the Sn-20In-2Ag-0.5Cu solder joints (5.4 N). It is also higher than the traditional Sn-37Pb solder joints (8.7 N) reported by another study.[21] After aging the Sn-3.8Ag-0.7Cu solder joints for 100 h at 100°C and 150°C, this strength will drop to 8.8 N and 7.8 N, respectively. With further increase of the aging time at 100°C and 150°C, the ball shear strengths decline linearly at about 1.5×10^{-3} N/h and 7.8×10^{-4} N/h, respectively. Prolonged aging for 1,000 h at 100°C and 150°C causes the strength to drop to 7.5 N and 7 N, respectively. Even in this case, the Sn-3.8 Ag-0.7Cu solder joints still claim a relatively higher strength in comparison with the traditional Sn-37Pb BGA packages after aging at 75°C for 500 h (6.25 N).[21] Aging treatments executed at 75°C and 115°C for Sn-20In-2Ag-0.5Cu solder BGA packages cause the joint strengths to decrease continuously with time. After a prolonged aging period of 1,000 h, the strengths drop to 4.2 N and 3.2 N for the aging temperatures of 75°C and 115°C, respectively.

Table II. Ball Shear Strengths of the Sn-3.8Ag-0.7Cu and Sn-20In-2Ag-0.5Cu Solder Joints in Ball Grid Array Packages under Various Aging Conditions

	Ball Shear Strength (N)			
	Sn-3.8Ag-0.7Cu		Sn-20In-2Ag-0.5Cu	
Aging Time (h)	100°C	150°C	75°C	115°C
100	8.8	7.8	5.1	4.7
300	8.6	7.4	4.9	4.2
500	8.4	7.6	5.0	4.5
700	8.0	7.2	4.5	3.7
1,000	7.5	7.0	4.2	3.2

As-reflow strength: 10.4 N (Sn-3.8Ag-0.7Cu), 5.4 N (Sn-20In-2Ag-0.5Cu).

After ball shear testing, fractography of the solder joints is observed via SEM. Figure 15 shows that the Sn-3.8Ag-0.7Cu BGA solder joints exhibit ductile-dimple fracture in the solder balls. The Sn-3.8Ag-0.7Cu BGA solder has a solder/pad interface stronger than the solder matrix after prolonged aging treatments at 100°C and 150°C. Therefore, the strength of the solder joint is determined by the strength of the solder matrix. Because the as-reflowed Sn-3.8Ag-0.7Cu solder balls contain many Ag_3Sn fine particles and a few Cu_6Sn_5 precipitates, both of which have a strengthening effect on the solder matrix, a maximum strength of 10.4 N can be obtained. However, the dissolution of the Cu_6Sn_5 precipitates in the solder matrix after aging causes a sharp decline of the ball shear strength. Despite this degradation effect, the Ag_3Sn precipitates are still capable of reinforcing the Sn-3.8Ag-0.7Cu solder matrix. With the increase of aging temperature and time, the number of Ag_3Sn particles decreases because of coarsening, leading to a further decline of the ball shear strength. Although the $(Cu_{0.70}Ni_{0.14}Au_{0.16})_6Sn_5$ intermetallic compounds float into the Sn-3.8Ag-0.7Cu solder matrix after prolonged aging, they will join with the coarsened Ag_3Sn phase to form intermetallic chains or clusters locally, which still fail to render a strengthening effect on the solder matrix.

Figure 16 shows the fractography of the Sn-20In-2Ag-0.5Cu solder joints in BGA packaging after ball shear tests. Figure 8a and b show that ductile-dimple fracture occurred in the solder balls of the specimens after reflow and aging at 75°C. Similar ductile fracture is also observed in the solder matrix after the Sn-20In-2Ag-0.5Cu BGA packages undergo aging at 115°C over a duration shorter than 500 h, as shown in Fig. 16c. However, aging treatments at 115°C for 700 h and 1,000 h can cause brittle fracture at the location of the $(Ni_{0.85}Cu_{0.15})(Sn_{0.71}In_{0.29})_2$ intermetallic layer (IM2b), as evidenced in Fig. 16d and e. The results show that the newly appeared IM2b intermetallic compound in Sn-20In-2Ag-0.5Cu solder joints is much more brittle and weaker than the original IM1b intermetallics. In the previous study on the Sn-20In-0.8Cu BGA packages after prolonged aging at 115°C for 700 h, the brittle nature of the $(Ni_{0.91}Cu_{0.93})_3(Sn_{0.77}In_{0.23})_2$ intermetallic compounds formed ahead of the Ni layer also initiated fracture in this brittle intermetallic phase accompanied by a low joint strength.[19]

CONCLUSIONS

The interfacial reactions of Sn-3.8Ag-0.7Cu and Sn-20In-2Ag-0.5Cu solder balls with Au/Ni surface finishes in BGA packages during reflow and aging treatments were investigated. After reflow, scallop-shaped intermetallic compounds $(Cu_{0.70}Ni_{0.28}Au_{0.02})_6Sn_5$ (IM1a) and $(Cu_{0.76}Ni_{0.24})_6(Sn_{0.86}In_{0.14})_5$ (IM1b) formed at the solder/pad interfaces of Sn-3.8Ag-0.7Cu and Sn-20In-2Ag-0.5Cu BGA packages, respectively. Further aging at 100°C and 150°C for Sn-3.8Ag-0.7Cu solder joints leads to the appearance of a new $(Cu_{0.70}Ni_{0.14}Au_{0.16})_6Sn_5$ intermetallic phase (IM2a) ahead of the aforementioned IM1a intermetallics. The formation of both intermetallics is caused by the dissolution of Cu_6Sn_5 precipitates originally contained in the solder matrix and their further reaction at the interfaces with the Ni and Au atoms of the Au/Ni surface finishes. In this case, the solder balls are strengthened by the Ag_3Sn precipitates. During aging treatment, the thickness of IM1a intermetallics diminishes slightly, while the IM2a intermetallic compounds grow at a more rapid pace with an increase of aging time. Kinetics analysis shows that the growth of IM2a in Sn-3.8Ag-0.7Cu solder joints is diffusion-controlled. After prolonged aging at 150°C, the IM2a intermetallic compounds partially spall away from IM1a and float into the solder matrix.

During the aging of Sn-20In-2Ag-0.5Cu solder joints at 75°C and 115°C, interfacial-intermetallic IM1b grows very slowly during the aging at 75°C and 115°C, with a portion of the IM1b intermetallics spalling from the interfaces. After prolonged aging at 115°C over durations longer than 500 h, a new intermetallic layer $(Ni_{0.85}Cu_{0.15})(Sn_{0.71}In_{0.29})_2$ (IM2b) is formed between IM1b intermetallics and the Ni layers of the Au/Ni surface finishes.

The as-reflowed Sn-3.8Ag-0.7Cu solder joints in BGA packaging possess a high shear strength of

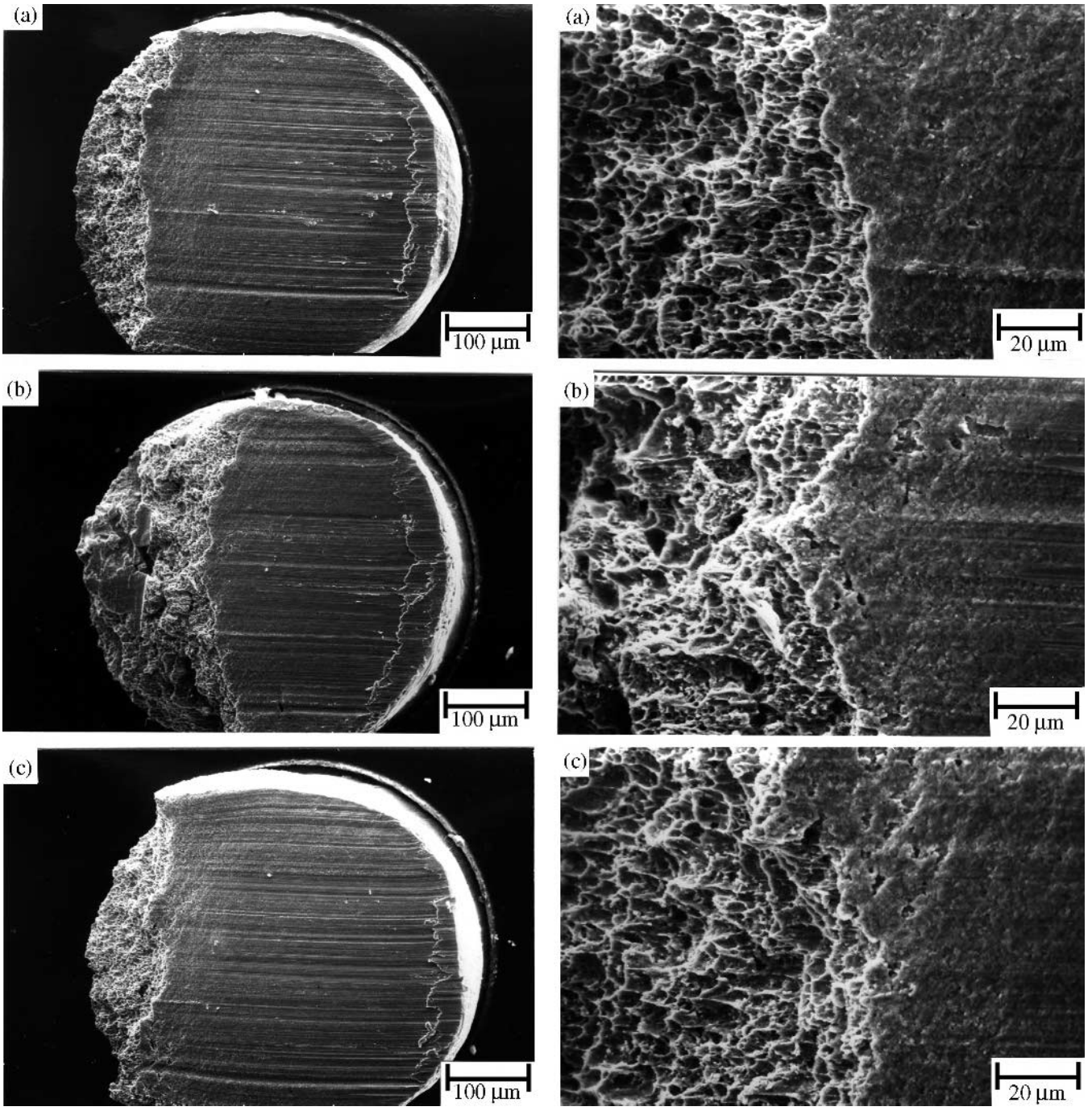

Fig. 15. Fractography of the Sn-3.8Ag-0.7Cu solder joints in BGA packaging after ball shear tests: (a) after reflow; (b) 100°C aging, 1,000 h; and (c) 150°C aging, 1,000 h.

10.4 N, which drops drastically to 8.8 N and 7.8 N after aging tests for 100 h at 100°C and 150°C, respectively. The joint strengths decline linearly at about 1.5×10^{-3} N/h and 7.8×10^{-4} N/h with further increases of the aging time at 100°C and 150°C, respectively. After ball shear tests of Sn-3.8Ag-0.7Cu BGA packages, fractography shows that the solder joints of all specimens under various conditions in this study fractured in the solder balls with ductile-dimple failure characteristics.

The ball shear strength of the Sn-20In-2Ag-0.5Cu solder joints in BGA packaging after reflow is 5.4 N, which declines with time in aging treatments. The ball-shear-tested specimens after reflow and aging at 75°C are fractured in the solder matrix with dimple characteristics. Such ductile fractures also occur to the solder joints after aging at 115°C over durations below 500 h. However, after aging at 115°C for 700 h and 1,000 h, the fracture location for such Sn-20In-2Ag-0.5Cu solder joints

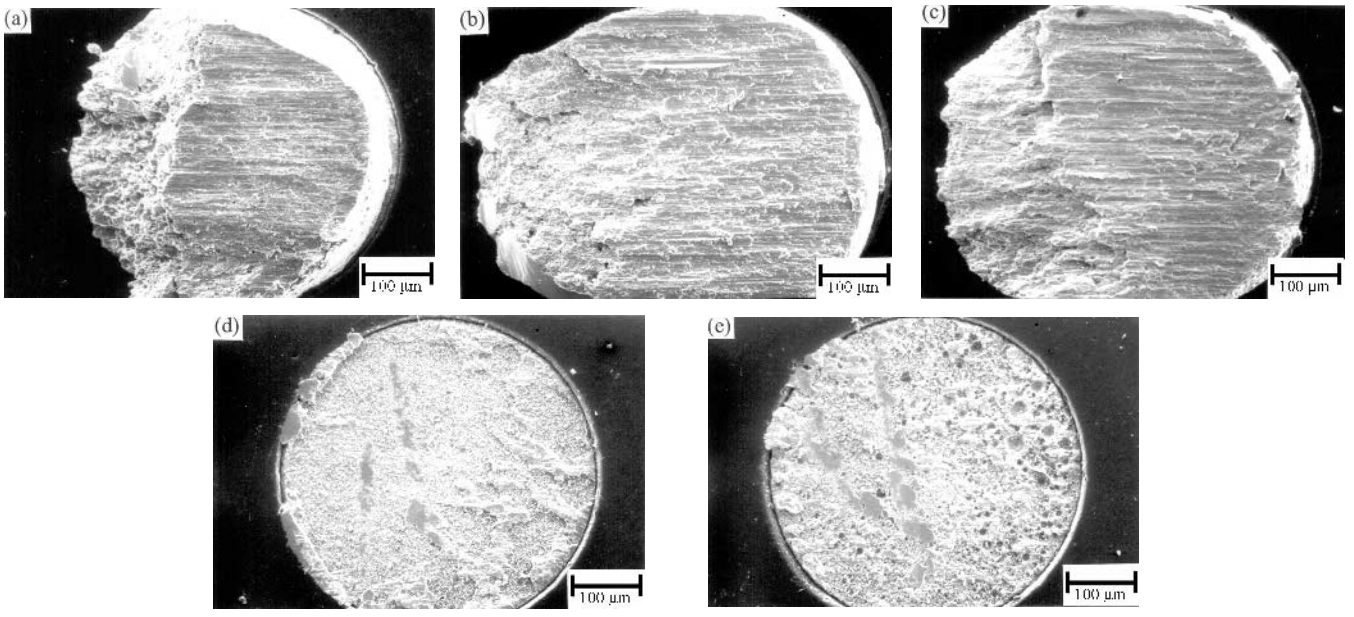

Fig. 16. Fractography of the Sn-20In-2Ag-0.5Cu solder joints in BGA packaging after ball shear tests: (a) after reflow; (b) 75°C aging, 1,000 h; (c) 115°C aging, 500 h; (d) 115°C aging, 700 h; and (e) 115°C aging, 1,000 h.

are transferred to the brittle IM2b intermetallic layer.

ACKNOWLEDGEMENTS

Special thanks to the National Science Council, Taiwan, for sponsoring this research under Grant No. NSC-91-2216-E002-037.

REFERENCES

1. K. Zeng and K.N. Tu, *Mater. Sci. Eng.* R38, 55 (2002).
2. A.M. Minor and J.W. Morris, Jr., *J. Electron. Mater.* 29, 1170 (2000).
3. P.G. Kim and K.N. Tu, *J. Appl. Phys.* 80, 3822 (1996).
4. M.R. Marks, *J. Electron. Mater.* 31, 265 (2002).
5. C.E. Ho, Y.M. Chen, and C.R. Kao, *J. Electron. Mater.* 28, 1231 (1999).
6. C.L. Yu (Ph.D. thesis, National Taiwan University, 2002).
7. P.G. Kim, J.W. Jang, T.Y. Lee, and K.N. Tu, *J. Appl. Phys.* 86, 6746 (1999).
8. K. Zeng, V. Vuorinen, and J.K. Kivilahti, *Proc. 51st Electronic Components and Technology Conf.* (Piscataway, NJ: IEEE, 2001), pp. 685–690.
9. F. Zhang, M. Li, C.C. Chum, and Z.C. Shao, *J. Electron. Mater.* 32, 123 (2003).
10. L.S. Shiau, C.E. Ho, and C.R. Kao, *Soldering Surf. Mount Technol.* 14, 25 (2002).
11. T.L. Su, L.C. Tsao, S.Y. Chang, and T.H. Chuang, *J. Mater. Eng. Performance* 11, 481 (2002).
12. T.Y. Lee, W.J. Choi, K.N. Tu, J.W. Jang, S.M. Kuo, J.K. Lin, D.R. Frear, K. Zeng, and J.K. Kivilahti, *J. Mater. Res.* 17, 291 (2002).
13. J. Haimovich, *AMP J. Technol.* 3, 46 (1993).
14. Z. Mei and J.W. Morris, *J. Electron. Mater.* 21, 401 (1992).
15. Z. Mei and J.W. Morris, *J. Electron. Mater.* 21, 599 (1992).
16. D.M. Jacobson and D. Himpston, *Gold Bull.* 22, 9 (1989).
17. N.C. Lee, *Soldering Surf. Mount Technol.* 26, 25 (1997).
18. T.H. Chuang, S.Y. Chang, L.C. Tsao, W.P. Weng, and H.M. Wu, *J. Electron. Mater.* 32, 195 (2003).
19. M.J. Chiang, S.Y. Chang, and T.H. Chuang, *J. Electron. Mater.* 33, 34 (2004).
20. Y.H. Tseng (Ph.D. thesis, National Taiwan University, 2000).
21. C.L. Yu (Ph.D. thesis, National Taiwan University, 2002).